

Modelling Galaxy Formation at high z

Cedric Lacey¹, Carlton Baugh², Shaun Cole², Carlos Frenk²

¹*Theoretical Astrophysics Center, Juliane Maries Vej 30, 2100 Copenhagen Ø, Denmark*

²*Department of Physics, Science Laboratories, South Rd, Durham DH1 3LE, England*

Abstract. I describe a semi-analytical model for the formation and evolution of galaxies in hierarchical clustering models, and its predictions for the properties of the galaxy population at high z . The predictions are found to agree well with the observed properties of the Lyman break galaxies found at $z \sim 3$ by Steidel et al. . The models predict that the star formation rate per comoving volume should have peaked at $z \sim 1 - 2$, which also agrees well with recent observational data.

1 Introduction

Recent observations have begun to probe the population of normal galaxies at high redshift. In particular, the technique of using multi-colour surveys of faint galaxies to look for high- z objects with strong Lyman break features has revealed a large population of star-forming galaxies at redshifts $z \sim 3 - 5$, based both on ground-based [14] and HST [11] imaging. It is a challenge to theoretical models of galaxy formation to explain the numbers and properties of these young galaxies. I describe here some recent theoretical results on high- z galaxies based on semi-analytical galaxy formation models [3], which show that the properties of the observed galaxies agree remarkably well with predictions based on hierarchical clustering.

2 Semi-analytical models

The semi-analytical models are constructed as described in [5], [3]. There are several steps involved. (1) We start with an assumed comology and initial spectrum of density fluctuations. Dark matter halos form through hierarchical clustering and merging. We describe this by means of *merger trees*, constructed by a Monte Carlo method, which specify the complete formation and merging histories of present-day halo of different masses. The number density of halos of different masses is given by the Press-Schechter theory. (2) Within each halo, diffuse gas is assumed to be shock-heated to the virial temperature during the collapse of the halo, and then to cool radiatively. We calculate how much gas cools in any halo during its lifetime, defined as the time until its mass has doubled by merging, based on an assumed density profile. The gas which cools

settles into a rotationally supported disk, whose radius we calculate based on the initial angular momentum of the gas in the halo, derived from tidal torques. (3) The cold gas forms stars, on a timescale which is assumed to depend on the circular velocity of the galaxy. (4) Supernovae from massive stars reheat some of the gas, ejecting it back into the halo, at a rate which also depends on the circular velocity. This feedback effect strongly suppresses star formation in low mass galaxies. The dependences of the star formation and feedback rates on circular velocity are based on numerical simulations [13]. (5) In major halo mergers, when the halo mass doubles, the remaining gas in the halo is reheated to the new virial temperature. The largest galaxy becomes the new central galaxy, and the galaxies from the other halos become satellite galaxies, which then merge with the central galaxy if their dynamical friction timescales are less than the halo lifetime. In general, not all of the satellites will merge. Mergers between disk galaxies where the mass ratio exceeds a critical value (~ 0.3) form elliptical galaxies. The elliptical may grow a new disk by gas cooling and become a bulge in a spiral galaxy. (6) We calculate the luminosity evolution of the stellar populations using an updated version of the population synthesis model of Bruzual & Charlot [4]. From these models, we calculate the distributions of galaxy masses, luminosities, colours, sizes, circular velocities, morphologies etc, and how these evolve with redshift.

The adjustable parameters in the model (relating to star formation, feedback and merging) are fixed by comparison with observations of present-day galaxies. Results of the models for zero and low redshifts for various CDM-based cosmologies are given in [5], [8], [1], [2]. The models fit the observed properties of low- z galaxies (luminosity functions, colours, morphologies, number counts) fairly well.

3 Lyman break galaxies

Steidel et al. [14] discovered a population of normal galaxies at $3 \lesssim z \lesssim 3.5$, forming stars at rates $\sim 1 - 10 M_{\odot}/yr$, by measuring U_nGR colours for faint galaxies and looking for galaxies with a strong Lyman break feature at this redshift; the redshifts were then confirmed spectroscopically. The number of such galaxies was found to be $\approx 1400 deg^{-2}$ at $\mathcal{R}_{AB} < 25$. These galaxies presumably represent the progenitors of present-day galaxies soon after they formed, and so reproducing their properties is a crucial test of theoretical models. To perform this test, we have used our semi-analytical models to generate mock catalogues of galaxies covering all redshifts, including the effects of absorption by intervening gas, and then applied the same colour selection as Steidel et al. . We present here results for 2 CDM models, both normalized in σ_8 to match the number density of clusters at $z = 0$: an $\Omega = 1$ model, with $h = 0.5$, $\sigma_8 = 0.67$, $\Omega_b = 0.06$, and an $\Omega_0 = 0.3$, $\Lambda_0 = 0.7$ model, with $h = 0.6$, $\sigma_8 = 0.97$, $\Omega_b = 0.04$. For a Miller-Scalo IMF, these models predict respectively 900 and $3000 deg^{-2}$ Lyman break galaxies satisfying the Steidel et

al. colour and magnitude selection, similar to the observed value. These values are sensitive to the power spectrum normalization σ_8 , and to the IMF used. However, using a Salpeter IMF gives similar values. The predicted redshift distributions match the observed ones

Figure 1 shows some of the properties of Lyman break galaxies predicted for the two CDM models. The stellar masses are predicted to be $\sim 3 \times 10^9 - 10^{10} h^{-1} M_\odot$, depending on the cosmology, while the halo masses are predicted to be $\sim 10^{12} h^{-1} M_\odot$ in either case. The galaxies are predicted to be in halos with circular velocities $V_c \sim 250 - 450 \text{ km/s}$, very similar to the rotation velocities inferred observationally for these galaxies from the widths of saturated interstellar absorption lines [14]. The star formation rates are predicted to be $\sim 1 - 10 h^{-2} M_\odot \text{ yr}^{-1}$, which follows essentially from the observed \mathcal{R} magnitudes and the assumed IMF. We also predict colours $(\mathcal{R} - K)_{AB} \approx 0.5 - 1.0$, and small sizes, with half-light radii $\sim 0.5 h^{-1} \text{ kpc}$, both of these comparable to the observed values [14], [7]. The halo masses predicted for these galaxies are fairly large compared to the typical halo at $z \sim 3$, and as a consequence, the galaxies are predicted to be quite strongly clustered, with a bias $b \approx 4$ and a comoving correlation length $r_0 \approx 4 h^{-1} \text{ Mpc}$ (see Figure 2). This agrees with evidence for strong clustering in the observed redshift distribution found by [15].

The predicted properties of the star-forming galaxy population at $z \sim 3$ are thus in good agreement with what is known observationally. The Lyman break galaxies found by Steidel et al. are predicted to evolve into $L \sim L_*$ ellipticals and spirals at the present day, and to be found preferentially in large groups and clusters at $z = 0$.

4 Cosmic Star Formation History

The global star formation history of the universe is a fundamental quantity in galaxy formation studies. Galaxy formation models based on CDM have typically predicted that most of the stars form fairly late, with a median formation redshift $z < 1$ according to [9], [5]. It has recently become possible to estimate the global star formation history out to $z \lesssim 5$ observationally, using measurements of the $H\alpha$ and UV luminosity functions of galaxies at different redshifts [6], [10], [12]. Significant uncertainties still remain, notably in the form of the IMF, the correction for galaxies below the luminosity limits of the surveys, and in the effects of dust. However, it seems that a consistent picture is emerging. The observations indicate that the star formation rate per comoving volume peaked at $z \sim 1 - 2$, and this agrees very well with the predictions of both of our CDM models, as shown in Figure 3. According to the models, less than 10% of the stars formed at $z > 3$. Note that the star formation history for $\Omega = 1$ shown here is essentially identical to that predicted in an earlier version of the model by [5]. The predictions for the SFR history are sensitive to the parameters describing SFR and feedback, but

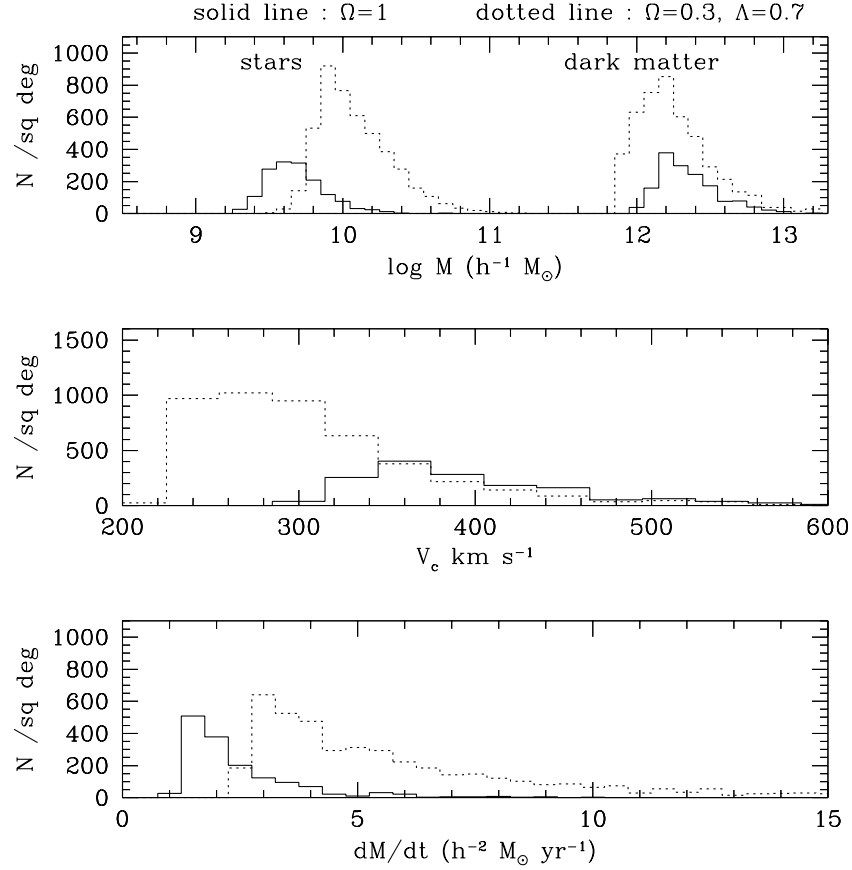


Figure 1: Predicted properties of Lyman break galaxies at $z \sim 3$, selected according to Steidel et al. U_nGR colour criteria and with $\mathcal{R}_{AB} < 25.0$. Results are shown for 2 CDM models, $\Omega = 1$ (solid lines) and $\Omega_0 = 0.3, \Lambda_0 = 0.7$ (dotted lines). Histograms show number of objects per bin per sq.deg. Top panel shows distributions of stellar and dark halo masses, middle panel shows halo circular velocities, and bottom panel shows star formation rates.

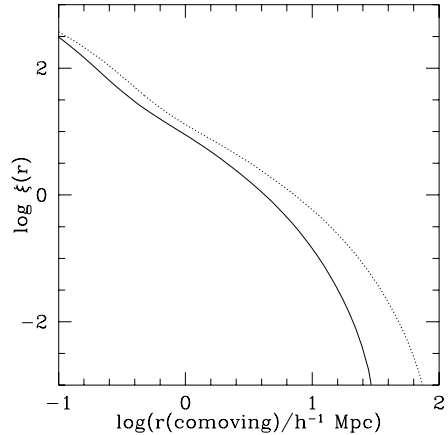


Figure 2: Predicted clustering of Lyman break galaxies at $z \approx 3$. Galaxies selected according to Steidel et al. . The spatial correlation function in comoving coordinates is shown for the $\Omega = 1$ (solid line) and $\Omega_0 = 0.3$, $\Lambda_0 = 0.7$ (dotted line) models.

these were chosen as in [5] to fit observations of present-day galaxies, without any knowledge of the observational data in Figure 3. Our model results are therefore real predictions, and the observational comparison represents a real success of the model.

References

- [1] Baugh, C.M., Cole, S., & Frenk, C.S., 1996, MNRAS 282, L27
- [2] Baugh, C.M., Cole, S., & Frenk, C.S., 1996, MNRAS 283, 1361
- [3] Baugh, C.M., Cole, S., Frenk, C.S., & Lacey, C.G., 1997, ApJ submitted (astro-ph/9703111)
- [4] Bruzual, G., & Charlot, S., 1993, ApJ 405, 538
- [5] Cole, S., et al. 1994, MNRAS 271, 781
- [6] Gallego, J., Zamorano, J., Aragon-Salamanca, A., REgo, M., 1995, ApJ 455, L1
- [7] Giavalisco, M., Steidel, S., Macchetto, F.D., 1996, ApJ 470, 189.
- [8] Heyl, J.S., Cole, S., Frenk, C.S., & Navarro, J.F., 1995, MNRAS 274, 755
- [9] Lacey, C.G, Guiderdoni, B., Rocca-Volmerange, B., & Silk, J., 1993, ApJ 402, 15
- [10] Lilly, S.J., LeFevre, O., Hammer, F., & Crampton, D., 1996, ApJ 460, L1
- [11] Madau, P., et al. 1996, MNRAS 283, 1388
- [12] Madau, P. astro-ph/9612157
- [13] Navarro, J.F., & White, S.D.M., 1993, MNRAS 265, 271.
- [14] Steidel, C., et al. 1996, ApJ 462, L17
- [15] Steidel, C., et al. 1997, ApJ in press (astro-ph/9708125)

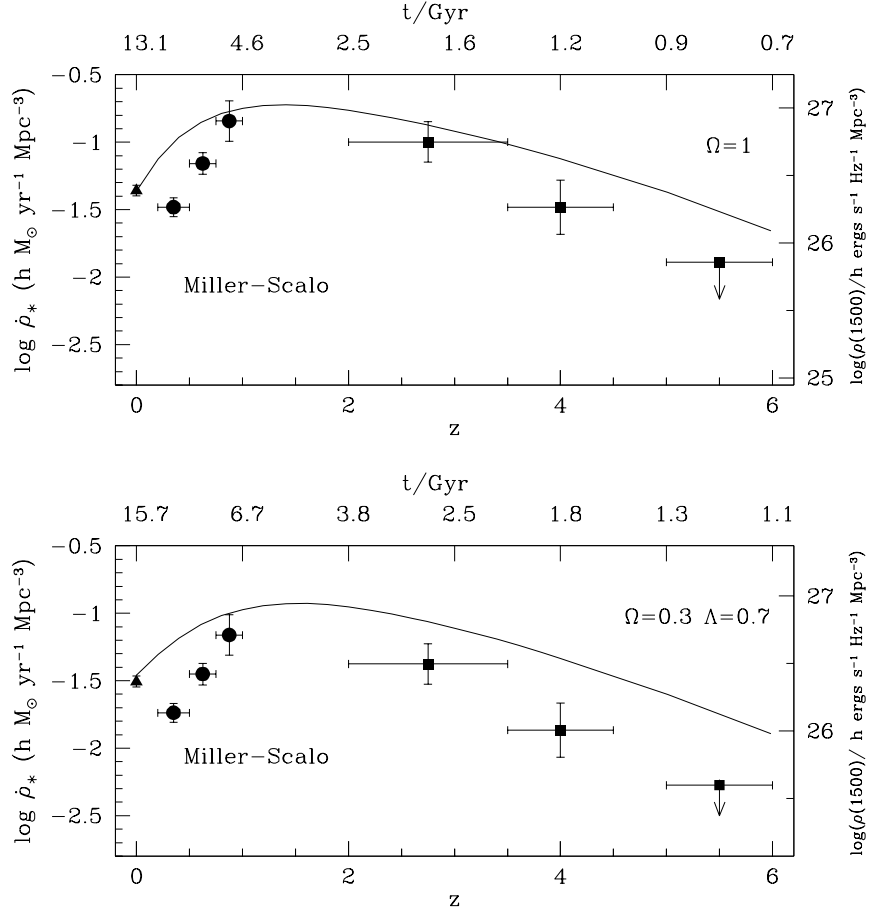


Figure 3: Cosmic star formation history. The 2 panels show the predicted star formation rate per comoving volume vs. redshift for our 2 CDM models, compared to observational data from [6], [10], [12]. The observational data have been converted to star formation rates using the same IMF as in the models.